Journal of Molecular and Cellular Cardiology 72 (2014) 263–272

Contents lists available at ScienceDirect

Journal of Molecular and Cellular Cardiology

journal homepage: www.elsevier.com/locate/yjmcc

Original article

Transcriptome profiling reveals that the SM22α-regulated molecular pathways contribute to vascular pathology

Rong Chen [a], Fan Zhang [a], Li Song [a,b], Yanan Shu [a], Yanling Lin [a], Lihua Dong [a], Xi Nie [a], Dandan Zhang [a], Peng Chen [a], Mei Han [a,*]

[a] Department of Biochemistry and Molecular Biology, College of Basic Medicine, Key Laboratory of Medical Biotechnology of Hebei Province, Key Laboratory of Neural and Vascular Biology of Ministry of Education, Hebei Medical University, Shijiazhuang 050017, PR China

[b] Department of Biochemistry and Molecular Biology, National Laboratory of Medical Molecular Biology, Institute of Basic Medical Sciences, Chinese Academy of Medical Sciences and Peking Union Medical College, 5 Dong Dan San Tiao, Beijing 100005, PR China

ARTICLE INFO

Article history:
Received 31 January 2014
Received in revised form 20 March 2014
Accepted 4 April 2014
Available online 13 April 2014

Keywords:
Transcriptome profiling
SM22α
NF-κB
Vascular inflammation
Atherosclerosis

ABSTRACT

Smooth muscle cell marker, SM22α, was down-regulated in the pathogenesis of arterial diseases including atherosclerosis, restenosis and abdominal aortic aneurysms. However, the question still exists whether this down-regulation actively contributes to the pathogenesis of vascular diseases. In an ongoing effort to understand the role of SM22α, here we explored transcriptome profiling by RNA-Seq from arteries of SM22α$^{-/-}$ and SM22α$^{+/+}$ mice. Analysis revealed that the most enriched pathways caused by SM22α-knockout were hematopoiesis, inflammation and lipid metabolism, respectively, and NF-κB, RXRα and PPARα were the major upstream regulators. The candidate genes involved in inflammation and lipid metabolism were clustered in atherosclerosis. Thus we suspected that the molecular basis in SM22α$^{-/-}$ mice was already prepared for the initiation of atherosclerosis. Further analysis suggested the up-regulated TNF caused NF-κB pathway activation. Our results showed loss of SM22α exacerbated TNF-α-mediated NF-κB activation and increased the expression levels of ApoCI *in vitro*, while overexpression of SM22α suppressed TNF-α-mediated NF-κB activation. In addition, disruption of SM22α enhanced injury-induced neointimal hyperplasia, and increased expression levels of molecules related with cellular adhesion and extracellular matrix degradation. Taken together, these findings not only suggested down-regulation of SM22α can actively contribute to the pathogenesis of atherosclerosis from the molecular basis, but also further confirmed that the vascular cells of SM22α$^{-/-}$ mice may become more sensitive to extracellular stimulation, increasing its tendency to develop vascular diseases. Meanwhile, rescuing SM22α expression may provide a novel therapeutic strategy for arterial diseases.

1. Introduction

Cardiovascular diseases are the leading cause of mortality among patients throughout the world. Vascular smooth muscle cells (VSMCs) undergo remarkable phenotypic remodeling during vascular disease, such as atherosclerosis, diabetic macroangiopathy and restenosis [1,2]. They have a unique repertoire of contractile proteins which are required for their contractile function, and used as markers of differentiated smooth muscle cells [3]. These markers include SM α-actin [4], calponin, smooth muscle 22 alpha (SM22α) [5], SM myosin heavy chain (MHC) [6], and smoothelin [7]. All of these markers have highly correlation with all the physiological functions and pathological changes during vascular diseases. For example, loss of SM α-actin leads to VSMCs hyperplasia *in vivo* and *in vitro* [8]; calponin-1 is an actin-binding protein which is similar with SM22α and its degradation would result in decreased vascular contractile response [9]; MHCs expression is decreased in human coronary arteries after the fifth decade [10] and smoothelin-B deficiency can reduce vascular contractility and cardiac hypertrophy in mice [11].

SM22α, also named transgelin, is a 22 kDa protein abundant in contractile SMCs, and physically associates with actin filament bundles. The expression of SM22α is down-regulated in vascular diseases including atherosclerosis [12], abdominal aortic aneurysms [13] and hypotension [14]. Moreover, decreased expression of SM22α has been widely reported in many solid tumors, such as breast cancer [15], prostate cancer [16] and colorectal cancer [17], which may be an important early event of angiogenesis in tumor progression. Loss of SM22α in apolipoprotein E knockout (ApoE$^{-/-}$) mice led to enlarged atherosclerotic lesions [18]. Disruption of SM22α promoted arterial inflammation and chondrogenic conversion of VSMCs through activation of ROS-mediated NF-κB pathways [19,20]. Our recent studies revealed that the overexpression of SM22α inhibited VSMCs proliferation and neointimal formation induced by balloon injury *via* blockade of the Ras-ERK1/2 signaling

* Corresponding author. Tel.: +86 31186265639; fax: +86 31186265557.
E-mail address: hanmei@hebmu.edu.cn (M. Han).

http://dx.doi.org/10.1016/j.yjmcc.2014.04.003

pathway [21]. More recently, we demonstrated that SM22α, as a PKCδ-regulating and PKCδ-regulated adaptor protein, modulated vascular oxidative stress *in vitro* and *in vivo* through PKCδ-p47^{phox} axis *via* itself phosphorylation at Ser 181 site [22]. All of these literatures suggest a strong correlation between decreased expression of SM22α and vascular diseases. However, the question still exists whether this decreased expression of SM22α actively contributes to the pathogenesis of vascular diseases.

In this study, we generated the aortic transcriptomes of SM22α$^{-/-}$ and SM22α$^{+/+}$ mice by RNA-Seq (RNA-Sequencing) to reveal the function and regulatory mechanism of SM22α. This whole transcriptome comparison can provide a starting point for understanding the pathogenesis of vascular diseases related to SM22α. Also, blocking the decrease of SM22α may supply a novel strategy for dealing with arterial diseases.

2. Material and methods

2.1. Ethics statement

All animal experiments were reviewed and approved by the Institutional Animal Care and Use Committee of Animal Science and Technology, Hebei medical University and performed in accordance with the Regulations for the Administration of Affairs Concerning Experimental Animals (China, 1988).

2.2. Breeding of transgenic mice

The SM22α$^{-/-}$ mouse line (B6.129S6-*Tagln*$^{tm2(cre)Yec}$/J) which has a Cre-recombinase gene inserted into the endogenous transgelin (SM22α) locus was purchased from The Jackson Laboratory. SM22α-CreKI heterozygous and homozygous mice are fertile and this mutation results in a loss of function of the targeted gene. Cre-recombinase activity is shown in adult smooth muscle cells (such as arteries, veins, and visceral organs) and cardiac myocytes. All of the born mice were maintained under standard animal housing conditions with a 12 h light/dark cycle (light on 7 a.m.), temperature 22 °C, and given standard chow and water *ad libitum*. Mouse tail genotyping was performed before used. Thoracoabdominal arteries were collected from eight male SM22α$^{-/-}$ mice and littermate wild controls (12 weeks) after fasted for 8–12 h respectively. Then, the adventitia and endothelium were quickly stripped and separated from the thoracic aortas in ice cold RNase-free PBS. The harvested tissues were placed in RNA*later* (Ambion®) overnight at 4 °C and then transferred to −80 °C in preparation for RNA-seq analysis.

2.3. RNA-seq data generation

RNA-seq libraries were prepared in accordance with Illumina's sample preparation protocol. The libraries were sequenced onto an Illumina HiSeq2000 instrument and subjected to 100 cycles of paired-end (2 × 100 bp) sequencing. The processing of fluorescent images into sequences, base-calling and quality value calculations were performed using the Illumina data processing pipeline (version 1.8). Before assembly, high-quality clean reads were generated using FASTX toolkit pipeline (version 0.0.13), then the resulting high-quality reads were mapped onto the UCSC (mm10) using Tophat (version: 2.0.6) [23]. Cufflinks v2.0.2 [24] was used to process the Tophat alignments. Additionally, the abundance of assembled transcripts was estimated and reported as fragments per kilobase of exon per million fragments mapped (FPKM). Finally, the program Cuffdiff was used to define differential expression genes as a gene set for next analysis. All of the above processes were performed at Shanghai Biotechnology Corporation.

2.4. Functional annotation of differential expression genes by DAVID and PANTHER

The database for annotation, visualization, and integrated discovery (DAVID) v6.7 [25] was used to interpret the differential expression genes data. DAVID is a group of web-based tools that identify enriched biological themes and gene ontology (GO) terms, group functionally related genes, and cluster annotation terms for large gene lists [26]. The differential expression genes Entrz Gene IDs were converted to official gene symbols and then used for functional clustering and enrichment analysis. The functional annotation clustering algorithm was used to generate a clustered, non-redundant report of related annotation terms, and groups of annotation clusters with EASE scores 0.1 were retained. Finally, DAVID pathway mapping allows a gene list to be superimposed on static pathway maps such as BioCarta and KEGG pathways. Differential expression genes were submitted to the DAVID functional annotation tool to explore enriched GO terms and pathways of BioCarta and KEGG. Protein classification of differentially expressed genes was analyzed by PANTHER (Protein Analysis Through Evolutionary Relationships) [27].

2.5. Analysis of differential expression genes by IPA software

Differential expression genes were uploaded in the IPA tool (Ingenuity® Systems, www.ingenuity.com) and subsequently performed canonical pathway, upstream regulator, and gene network and subnetwork analysis. First, canonical pathway analysis was based on the IPA library of canonical pathways. The significance of the association between each list and a canonical pathway was measured by Fisher's exact test. As a result, a *P*-value was obtained, determining the probability that the association between the genes in our data set and a canonical pathway can be explained by chance alone. Second, based on previous knowledge of expected effects between transcriptional regulators and their target genes stored in the Ingenuity® Knowledge Base, upstream regulator analysis of differential expression genes was performed. Prediction of activation/suppression state for each transcription factor based on two statistical measures: an overlap *P*-value and an activation *Z*-score. *Z*-score was calculated using the gene expression patterns of the transcription factor and its downstream genes. An absolute *Z*-score of ≥|2| was considered significant. A *P*-value was also calculated by Fisher's exact test indicating the statistical significance of genes in the dataset that are downstream of the transcription factors. We set a threshold of an overlap $P < 0.05$ to identify significant upstream regulators. Finally, we used the network modules in the IPA system to identify the network and subnetworks of our candidate gene list. These genes were clustered into several (sub) networks, based on their protein–protein interaction, regulation, and other relationships.

2.6. Quantitative real-time PCR (qRT-PCR)

Quantitative real-time PCR (qRT-PCR) was used to measure the mRNA expression levels of genes. The qRT-PCR was performed on 7300 Real Time PCR System (Applied Biosystems) using SYBR® Green Real-time PCR Master Mix (TaKaRa, China) with 18S rRNA as endogenous control genes. The PCR primer sequences are shown in Supplementary material (Table S1) and $2^{-\Delta\Delta Ct}$ method was used to determine the relative mRNA abundance for the surveyed samples.

2.7. Animal model preparation with partial ligation and histopathology analysis

We performed an animal diseases model by partial ligation of the left carotid artery on both SM22α$^{-/-}$ and wild type mice. The carotid artery ligation model used in this study was described elsewhere [28]. The specimen was obtained after ligation for 14 days fixed in 7.5% formalin, embedded in paraffin, and processed for routine histopathologic examination. Vertical sections (20 μm thick) were stained with hematoxylin and eosin (H&E). Immunostaining of sections were performed with primary antibodies against MCP-1 (1:400, cat. no. MBS551047, MyBioSource), MMP-2 (1:200, cat. no. sc-13595, Santa Cru), MMP-9 (1:200, cat. no. sc-6840, Santa Cru), ICAM-1 (1:400, cat. no. sc-8439, Santa Cru), VCAM-1 (1:400, cat. no. sc-8304, Santa Cru).

2.8. SiRNA transfection and Western blot

The cultured VSMCs were grown to 50–60% confluence, and then transfected with specific duplex siRNA, SM22α siRNA (siSM22α) (5′-GCU AGU GGA GUG GAU UGU ATT-3′ and 5′-UAC AAU CCA CUC CAC UAG CTT-3′), Scrambled siRNA (siCon) (5′-GCU AGA GUA GCG GUG AAU UCG TT-3′ and 5′-CGA AUU CAC CGC UAC UCU AGC TT-3′) served as a negative control, using Lipofectamine® RNAiMAX Transfection Reagent (Invitrogen) according to the manufacturer's protocol. After 24 h after transfection, VSMCs were treated with TNF-α (10 ng/ml) for 15 min. RIPA buffer was used to lyse VSMCs (50 mM Tris–Cl, pH 7.5, 1% NP-40, 0.5% Na-deoxycholate, 150 mM NaCl) and mice arteries (50 mM Tris–Cl, pH 7.5, 1% NP-40, 0.5% Na-deoxycholate, 0.05% SDS, 1 mM EDTA, 150 mM NaCl). The nuclear and cytoplasmic protein separation was performed by NE-PER Nuclear and Cytoplasmic Extraction Reagents (Thermo). The proteins were separated by 10% or 12% SDS-PAGE, and electro-transferred onto a PVDF membrane. Membranes were blocked with 5% non-fat milk in TBST for 2 h at room temperature, and incubated with primary antibodies against SM22α (1:1000, cat. no. ab14106, Abcam), p-IκBα (Ser32/36) (1:1000, cat. no. 9246, Cell Signaling), IκBα (1:500, cat. no. 1130-1, Epitomics), NF-κB (1:500, cat.no. 622602, BioLegend), ApoCI (1:300, cat.no. AB21657b, BBI), β-actin (1:1000, cat.no. sc-47778, Santa Cruz) at 4 °C overnight, and then incubated with IRDye800® conjugated secondary antibody (1:20,000, Rockland) for 1 h, following scanning with the Odyssey Infrared Imaging System (LI-COR Biosciences), then the integrated intensity for each detected band was determined with the Odyssey Imager software (v3.0). The experiments were replicated at least three times.

2.9. Statistical analysis

Data analysis was performed by using SPSS version 17.0 (SPSS, Inc., Chicago, IL). Data were presented as the means ± s.d. Paired or unpaired data were performed by Student's *t* tests. Differences among groups were determined with one-way analysis of variance (ANOVA) with repeated measures. A *P*-value < 0.05 was considered significant.

3. Results

3.1. Differentially expressed genes generated by RNA-Seq

This SM22α-knockout mouse line was generated by knocking in the Cre-recombinase coding sequence into the endogenous SM22α gene locus on chromosome 9 *via* homologous recombination of embryonic stem cells. The results from Western blot and qRT-PCR demonstrated the ablation of SM22α (Figs. 1 A–B). Putative differentially expressed genes generated by RNA-Seq were identified (2 fold change cut-off). Using these criteria, there were a total of 1398 genes differentially expressed between SM22α$^{-/-}$ and wild-type mice. Of the 1398 differentially expressed genes, 959 (56.0%) genes were up-regulated while 439 (25.6%) genes were down-regulated. Although the majority of these significantly altered genes were protein-coding genes, approximately 315 (18.4%) were unknown/hypothetical function genes. We randomly selected 12 genes from those with both different expression patterns and interesting function, for qRT-PCR validation. Fold changes from qRT-PCR were compared with RNA-Seq expression analysis results (Fig. 1C).

Among the differentially expressed genes identified by SM22α-knockout, we found genes such as hemoglobin (Hb), apolipoprotein C-I (ApoCI) and G0/G1 switch gene 2 (G0s2) were highly expressed (Table 1). Specially, ApoCI is one of the most highly expressed (based on FPKM value) and significantly changed genes caused by SM22α-knockout.

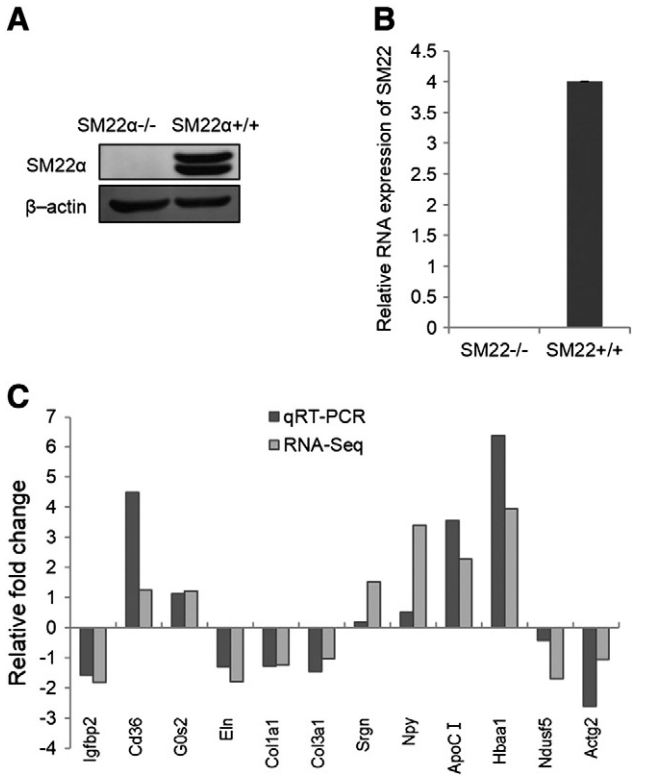

Fig. 1. Validation of the ablation of SM22α and comparison between RNA-Seq and qRT-PCR results. A-B, Western blot and qRT-PCR analysis of SM22α expression of vascular tissues from SM22α$^{-/-}$ and SM22α$^{+/+}$ mice. C, Comparison the fold change (log2) values of 12 selected transcripts using RNA-Seq and qRT-PCR.

3.2. Functional analysis of differentially expressed genes

The NCBI web-based functional annotation tool DAVID v 6.7 (Database for Annotation, Visualization and Integrated Discovery) was used to investigate functional associations of gene expression changes between SM22α$^{-/-}$ and SM22α$^{+/+}$. GO annotated differentially expressed genes mainly belonged to the three functional clusters (biological process, cellular component, and molecular function). The differentially expressed genes in the cluster of biological process were found to be mainly related to signal transduction, developmental processes, transport and cell communication (Fig. 2A). Cellular component GO terms of differentially expressed genes were related to the plasma membrane, synapse, extracellular region and cell junction (Table S2). The molecular function of GO terms were mainly involved of binding, catalytic activity, receptor activity and structure molecular activity (Fig. 2B).

Protein classification of differentially expressed genes using PANTHER (Protein Analysis Through Evolutionary Relationships), ranked receptors to the top, which is very similar to that obtained from molecular function GO database (Fig. S1). Subdivision of the receptors class showed “G-protein coupled receptor” and “cytokine receptor” were the top two class receptors (Fig. 2C). G-protein coupled receptors (GPCRs) are a large protein family of receptors that sense molecules outside the cell and activate inside signal transduction pathways and cellular responses. Important GPCRs found in differentially expressed genes included C-X-C chemokine receptor type 4 (CXCR4), adrenergic receptor, cadherin, neuropeptide Y receptor, platelet-activating factor receptor, probable C-C chemokine receptor type 3 (CCR3) and growth hormone secretagogue receptor type 1 (GHSR), which played vital functions in proliferation and migration of VSMCs [29–31]. The differentially expressed genes included the cytokine receptors related to coordinating immune and inflammatory responses, such as nerve growth factor receptor (NGFR), cytokine receptor-like factor 1 (CRLF1), CD48 antigen

Table 1
Top enriched differentially expressed genes identified by SM22α-knockout.

Up regulate genes		Down regulate genes	
Gene name	*Description*	*Gene name*	*Description*
ApoCI	Apolipoprotein C-I	Psmg4	Proteasome (prosome, macropain) assembly chaperone 4
Hba-a1	Hemoglobin alpha, adult chain 1	Nnmt	Nicotinamide N-methyltransferase
G0s2	G0/G1 switch gene 2	Eln	Elastin
Cd36	CD36 antigen	Ndufs5	NADH dehydrogenase (ubiquinone) Fe-S protein 5
Egr2	Early growth response 2	Ifit3	Interferon-induced protein with tetratricopeptide repeats 3
Arc	Activity regulated cytoskeletal-associated protein	Sparc	Secreted acidic cysteine rich glycoprotein
Ppbp	Pro-platelet basic protein	Tcap	Titin-cap
Igfbp2	Insulin-like growth factor binding protein 2	Fos	FBJ osteosarcoma oncogene
Scd1	Stearoyl-Coenzyme A desaturase 1	Adra1d	Adrenergic receptor, alpha 1d
Car3	Carbonic anhydrase 3	Lox	Lysyl oxidase
Ucp1	Uncoupling protein 1 (mitochondrial, proton carrier)	Hist2h3b	Histone cluster 2, H3b
Elovl6	ELOVL family member 6, elongation of long chain fatty acids (yeast)	Itih4	Inter alpha-trypsin inhibitor, heavy chain 4
Btnl9	Butyrophilin-like 9	Sgcg	Sarcoglycan, gamma (dystrophin-associated glycoprotein)
Srgn	Serglycin	Sec61g	SEC61, gamma subunit
Pnpla3	Patatin-like phospholipase domain containing 3	Lsm7	LSM7 homolog, U6 small nuclear RNA associated (S. cerevisiae)
Fasn	Fatty acid synthase	Ndufa2	NADH dehydrogenase (ubiquinone) 1 alpha subcomplex, 2
Cyp2e1	Cytochrome P450, family 2, subfamily e, polypeptide 1	Dsp	Desmoplakin

(CD48), interleukin-18 receptor (I18RA), I12R2, IL23R, IL9R, thrombopoietin receptor (TPOR) and neuronal cell adhesion molecule (NRCAM). In addition, transporter, hydrolase, signaling molecular and nucleic acid binding were also found as the major protein classes. Furthermore, protein classes more than 50 counts were also classified to enzyme modulators, transcription factors, cell adhesion molecules, cytoskeletal proteins, defense/immunity proteins, oxidoreductases and proteases.

To identify pathways in which differentially expressed genes were involved and enriched, pathway analysis was performed using KEGG, BioCarta and IPA, respectively. The most representative terms (higher level of the pathways) in KEGG included neuroactive ligand–receptor interaction, hematopoietic cell lineage and cytokine–cytokine receptor interaction. The most enriched pathways in BioCarta were associated with hematopoiesis-related cytokines, nuclear receptors involved in lipid metabolism and toxicity, and cytokines modulating inflammatory response (Fig. S2). IPA canonical pathway analysis allowed further insights into the molecular processes and pathways involved as SM22α-knockout. According to IPA, the specific enrichment pathways of differentially expressed genes were observed for LXR/RXR activation,

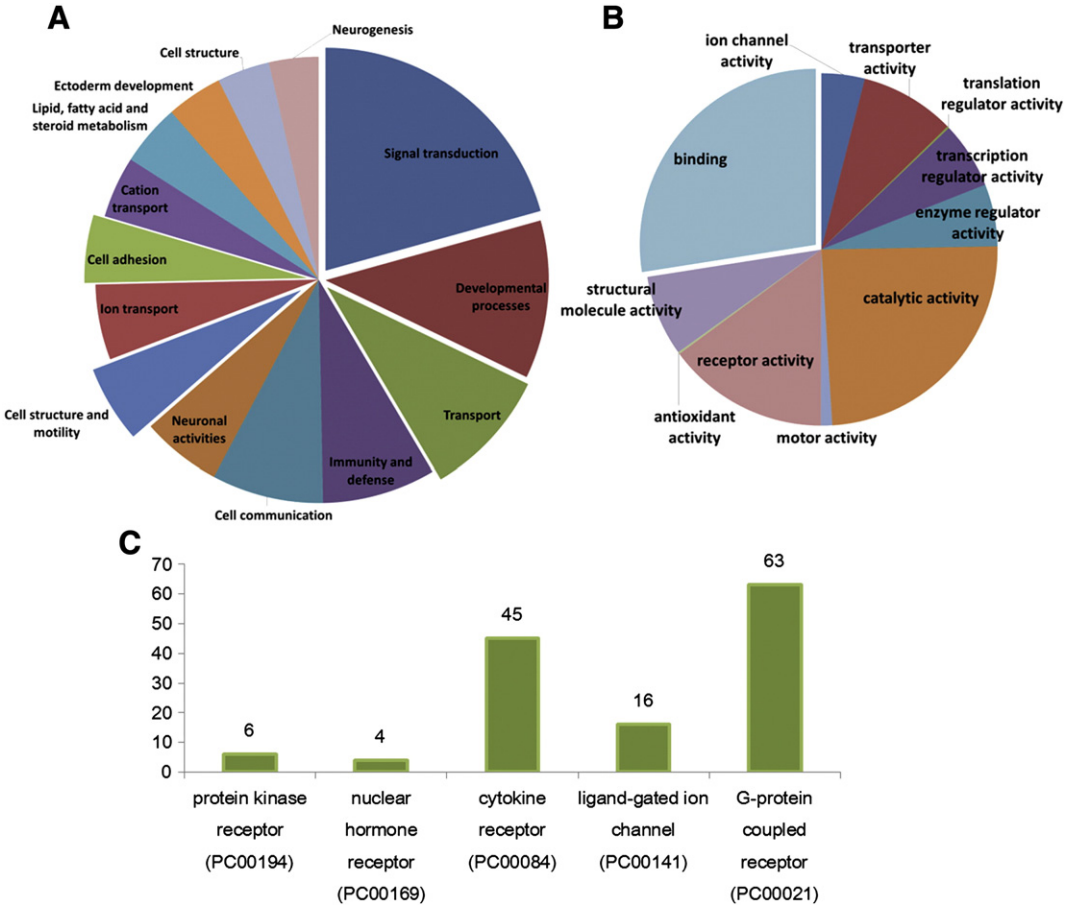

Fig. 2. Functional analyses of differentially expressed genes by DAVID and PANTHER. A, Representative GO terms of biological processes. B, Representative GO terms of molecular function. C, Subdivision of the receptors class by PANTHER showed "G-protein coupled receptor" and "cytokine receptor" were the top two class receptor.

atherosclerosis signaling, communication between innate and adaptive immune cells, dendritic cell maturation, altered T cell and B cell signaling in rheumatoid arthritis, calcium and amyotrophic lateral sclerosis signaling (Fig. 3). Further analysis of genes involved in these pathways were mainly G-protein coupled receptors (for example: CCR3, CCR4, adrenergic receptor) and cytokines (GM-CSF, IL-1α, IL-1β, IL3/6/11/18, TNF), implying that vascular cells were activated in SM22α$^{-/-}$ mice. Specifically, LXR/RXR pathway is mainly involved in cholesterol, fatty acid, and glucose homeostasis, including genes LXR, LPL, ApoCI, UDP glucuronosyltransferase 1 family polypeptide A3 (UGT1A3), IL-6, IL-1β and MCP-1. CCR3, CXCR4, collagen, IL-1, IL-6, MMP-13 and TNF-α were also clustered into atherosclerosis signaling pathway and participated in VSMC proliferation and foam cells activation. Overall, KEGG, BioCarta and IPA pathway analysis were all showed that the regulatory cytokines of hematopoiesis, inflammation and lipid metabolism were significantly enriched as top ranked pathways.

Upstream regulator analysis by IPA can identify potential regulatory nodes despite the levels of gene expression. By this analysis, we found 6 upstream regulators caused by SM22α-knockout (Table 2, Fig. S3). It showed that TNF was respectively the target gene of NF-κB, RXRα, JUN and KLF2. CXCR4 was activated by NF-κB, KLF2 and NUPR1. HLA-B was significantly up-regulated by both NF-κB and JUN. Col1a1 and Col3a1 were suppressed by NF-κB and NUPR1 respectively. These results suggest that the regulators of inflammation are activated in SM22α$^{-/-}$ mice.

We used the IPA system to examine the potential functional networks of differentially expressed genes, and found that these genes were clustered into 10 significant functional networks (Table S3). The main functional roles of these networks involved in cell signaling, lipid metabolism and cardiovascular disease. Diseases and functions analysis by IPA revealed that disease processes and biological functions caused by SM22α-knockout were mainly related to arteriosclerosis, atherosclerosis, hypotension, disorder of artery, occlusion of artery and vascular disease (Table S4, Fig. S4).

3.3. SM22α$^{-/-}$ mice showed characteristics of pro-atherosclerosis

A total of 45 genes were enriched in atherosclerosis predicted by IPA, indicating molecular changes by SM22α-knockout may have already initiated the early stage of atherosclerosis (Fig. 4A). Then we selected the enriched genes which are the markers of early atherosclerosis involved in inflammation (TNF, IL-18 [32]) and lipid translocation or metabolism (LPL, APOA2, Adiponectin, ApoCI) for further analysis. Quantitative real-time PCR showed that these gene expressions had a strong correlation with SM22α-knockout (Fig. 4B).

Atherosclerosis is virtually always accompanied of vascular inflammation during its early stage and the transcription factor NF-κB is a key regulator of inflammation [33]. Our data showed TNF was significantly up-regulated as SM22α-knockout and activated NF-κB pathway (Fig. 4C). To confirm the relationship between loss of SM22α and inflammation, we subsequently examined whether disruption/overexpression of SM22α affected TNF-α-mediated NF-κB activation in VSMCs. The results showed that knockdown of SM22α using specific siRNA increased phosphorylation and degradation of IκBα following TNF-α treatment (Figs. 5A–B). Disruption of SM22α activated NF-κB complex to translocate into the nucleus where it initiated gene expression, while overexpression of SM22α suppressed TNF-α-mediated NF-κB nucleus translocation (Figs. 5C–D). These results were in accordance with the above bioinformation analysis by IPA. Another important event in atherosclerosis is dysfunction of lipid metabolism. Network analysis revealed that lipoprotein ApoCI was a node molecular in cardiovascular diseases [34]. ApoCI was prominent expressed in the arteries of SM22α$^{-/-}$ mice compared with that in wild-type (Figs. 5E–F). Further, we found that suppression of SM22α by siRNA increased ApoCI expression levels in cultured rat VSMCs (Figs. 5G–H). Next, we performed serum lipid assay between SM22α$^{-/-}$ and SM22α$^{+/+}$ mice. The results showed the levels of triglycerides were up-regulated but a down-regulation of serum total cholesterol (Fig. S5). Meanwhile, genes enriched in fatty acid metabolism were clustered by IPA software analysis (Fig. S6).

3.4. SM22α$^{-/-}$ mice revealed increased tendency to develop vascular disease

Although SM22α$^{-/-}$ mice showed histologically indistinguishable from the tissues of their control littermates, pathway analysis were activated for hematopoiesis, inflammation and lipid metabolism from the above analysis. As inflammation and lipid metabolism are major risk incidents of atherosclerosis, we suspected that the molecular basis in SM22α$^{-/-}$ mice is already prepared for the initiation of atherosclerosis. Thus we next validated some candidate genes which expressed at the initiation stage of atherosclerosis. We also hypothesized that SM22α$^{-/-}$ mice may have an increased tendency to develop vascular

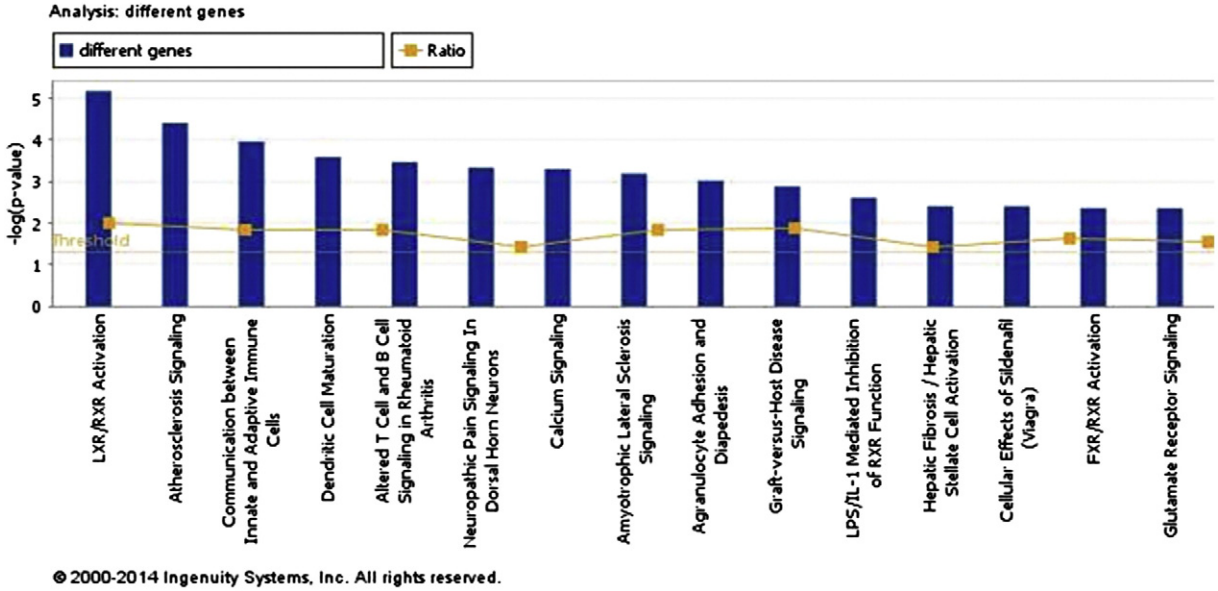

Fig. 3. Canonical Pathway analysis by IPA software.

Table 2
Upstream transcription regulator analysis by IPA.

Upstream regulator	Molecule type	Predicted activation	Activation Z-score
RELA	Transcription regulator	Activated	2.811
RXRA	Ligand-dependent nuclear receptors	Activated	2.720
PPARA	Ligand-dependent nuclear receptors	Activated	2.195
JUN	Transcription regulator	Activated	2.046
NUPR1	Transcription regulator	Activated	2.106
KLF2	Transcription regulator	Inhibited	−2.000

disease compared to the wild type based on the above molecular information analyzed by us.

The expression of molecules related with cellular adhesion and extracellular matrix degradation is the initiation step of vascular diseases such as atherosclerosis, neointimal thickening and aneurysm. We detected several molecules of differentially expressed genes based on GO analysis, which included monocyte chemoattractant protein-1 (MCP-1), intracellular cell adhesion molecule 1 (ICAM-1), vascular cell adhesion molecule 1 (VCAM-1) and matrix metalloproteinases (MMP-2, MMP-9) in SM22α$^{-/-}$ and SM22α$^{+/+}$ mice arteries by immunohistochemical staining. The results demonstrated that the expression of ICAM-1, MMP-2, MMP-9 and VCAM-1 were significantly elevated, while MCP-1 showed no obvious expression change both in SM22α$^{-/-}$ and SM22α$^{+/+}$ arteries (Figs. 6A–B).

Next, we established the model of neointimal formation using partial ligation of the left carotid arteries of both SM22α$^{-/-}$ and SM22α$^{+/+}$ mice. The intimal thickness in SM22α$^{-/-}$ mice was more than that of wild type mice after ligation for 14 days (Figs. 6C–D). The expressions of MCP-1, VCAM-1, ICAM-1, MMP-2 and MMP-9 were all exacerbated in the partial ligation model of SM22α$^{-/-}$ compared with SM22α$^{+/+}$ mice by immunohistochemistry staining (data not shown). ApoCI was up-regulated during carotid neointimal formation compared with normal arteries and loss of SM22α increased ApoCl expression, especially in the injured arteries by partial ligation (Fig. S7). These results may imply

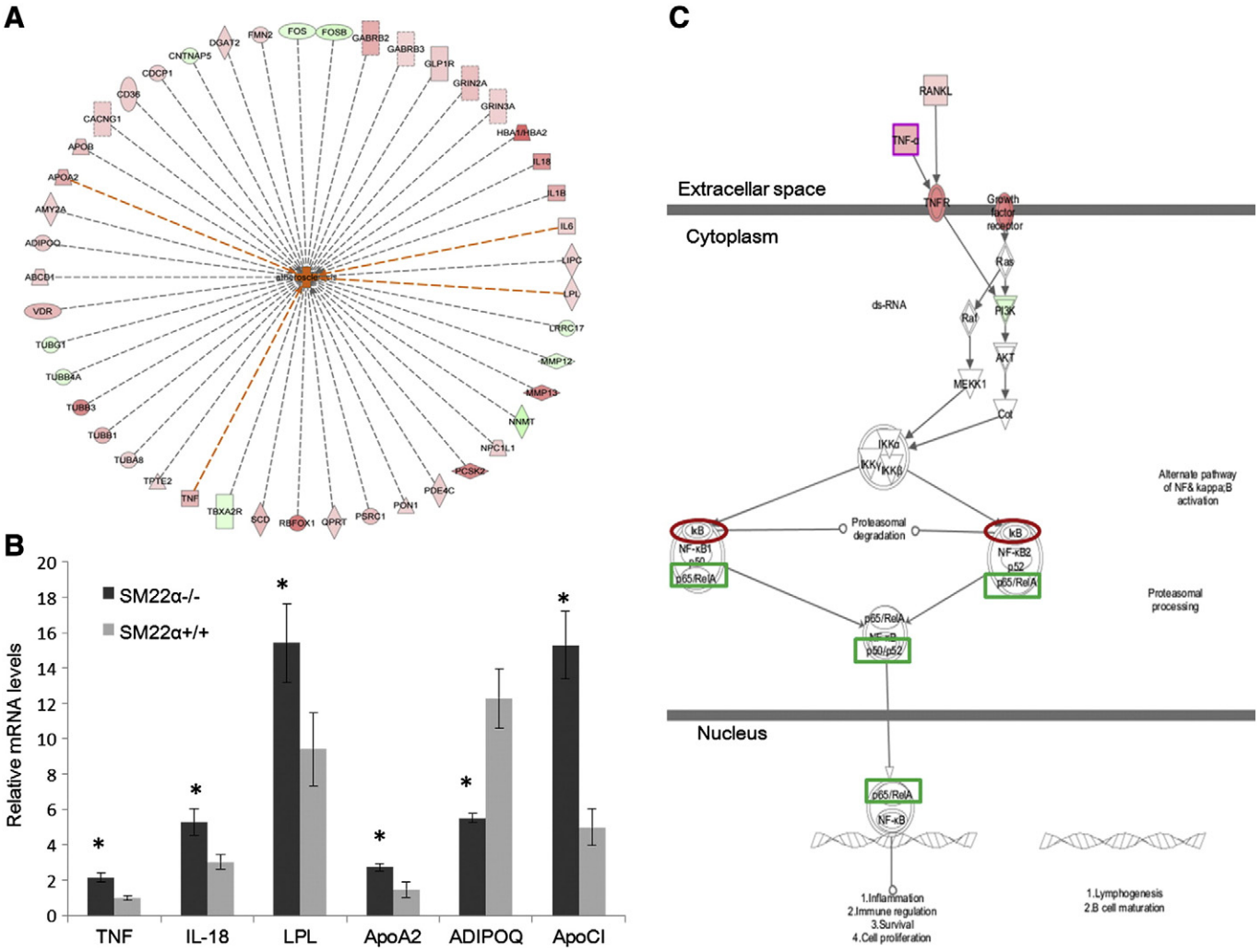

Fig. 4. Genes enriched in atherosclerosis predicted by IPA software and predicted NF-κB pathway activation. A, Diseases & functions analysis by IPA revealed that 45 genes were enriched in atherosclerosis as SM22α-knockout. B, Enriched genes were verified by qRT-PCR. Data are presented as the mean ± s.d. n = 3 mice per group. Student's *t* test was used to calculate the *P*-value. **P* < 0.05. C, TNF was significantly up-regulated as SM22α-knockout and activated NF-κB pathway.

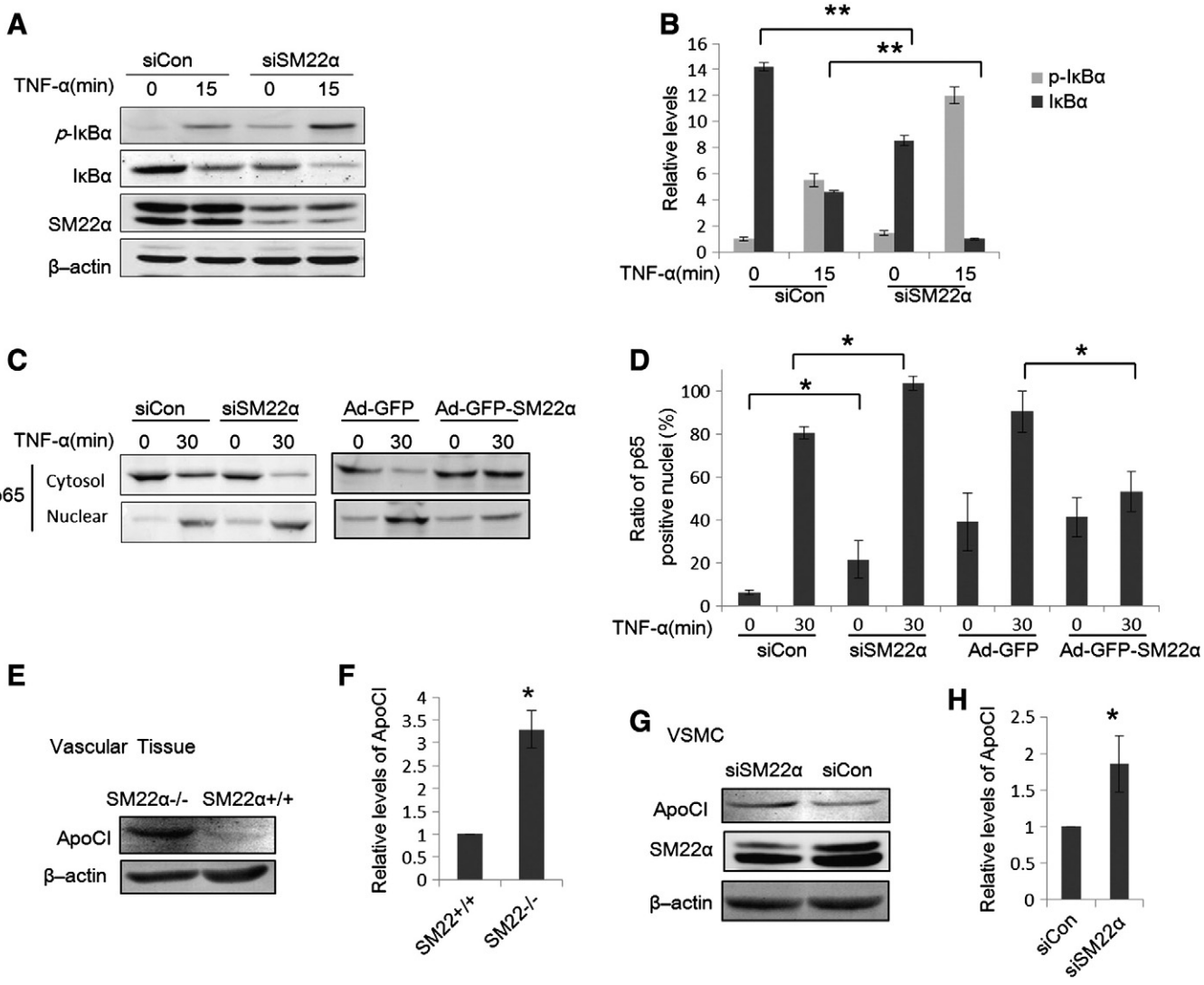

Fig. 5. SM22α$^{-/-}$ mice showed characteristics of pro-atherosclerosis. A-B, Western blots showed increased phosphorylation of IκB (Ser32/36) in siSM22α compared to siCon after treated with TNF-α (10 ng/ml) for 15 min. Data are presented as the mean ± s.d. ANOVA was applied to calculate the *P*-value. $^{**}P < 0.01$. C–D, Western blot showed disruption/overexpression of SM22α affected TNF-α-mediated nucleus translocations of NF-κB in VSMCs. Data are presented as the mean ± s.d. ANOVA was applied to calculate the *P*-value. $^{*}P < 0.05$. E–F, Western blot showed ApoCI expression in SM22α$^{-/-}$ and SM22α$^{+/+}$ mice arteries. Student's *t* test was used to calculate the *P*-value. $^{*}P < 0.05$. G–H, Western blot showed ApoCI expression in VSMCs transfected by siCon or siSM22. Student's *t* test was used to calculate the *P*-value. $^{*}P < 0.05$.

that disruption of SM22α influenced cellular adhesion and extracellular matrix degradation, enhanced the phenotype change of VSMCs and increased vascular response to injury.

4. Discussion

Previous studies showed that the dynamic expression levels of VSMCs marker, SM22α, had a high correlation with phenotypic remodeling of VSMCs and vascular injury, such as restenosis, atherosclerosis and hypertension. However, the question still exists whether disruption of SM22α actively contributes to the pathogenesis of vascular diseases. In order to gain comprehensive insight into the function of SM22α involved in vascular diseases, the present study investigated the different gene expression patterns in SM22α$^{-/-}$ mice using RNA-Seq. The up-regulated genes caused by SM22α-knockout were more than the down-regulated genes. This suggests that highly expressed genes in SM22α-knockout mice play relatively greater roles in determining VSMC phenotypes during vascular injury.

The most highly differentially expressed and changed gene is ApoCI. ApoCI is expressed in the liver, lung, skin, spleen, adipose tissue, central nervous system, kidney, brain, and has several roles in lipid metabolism [35]. ApoCI improved the presentation of LPS to macrophages *in vitro* and *in vivo*, thereby accelerated atherosclerosis after treatment with LPS [36]. Furthermore, ApoCI is the major plasma inhibitor of cholesteryl ester transfer protein (CETP) *via* inhibiting lipoprotein binding to the LDL and VLDL receptors. Nineteen pathways related to ApoCI enriched in 'phospholipid efflux' which is strongly associated with the atherosclerotic process [34,35,37]. Reports showed that mice with transgenic expression of human ApoCI in the liver and skin have strongly increased serum levels of cholesterol, triglycerides, and free fatty acids, indicative of a disturbed lipid metabolism [38]. Studies in humans and mice have also shown that increased expression of ApoCI results in combined hyperlipidemia with a more pronounced effect on triglycerides (TG) compared with total cholesterol (TC) [39]. ApoCI was found prominently elevated in the atheroma of the carotid and femoral arteries compared to non-atherosclerotic arteries [40]. ApoCI may contribute to the pathogenesis of atherosclerosis [41]. The elevated levels of

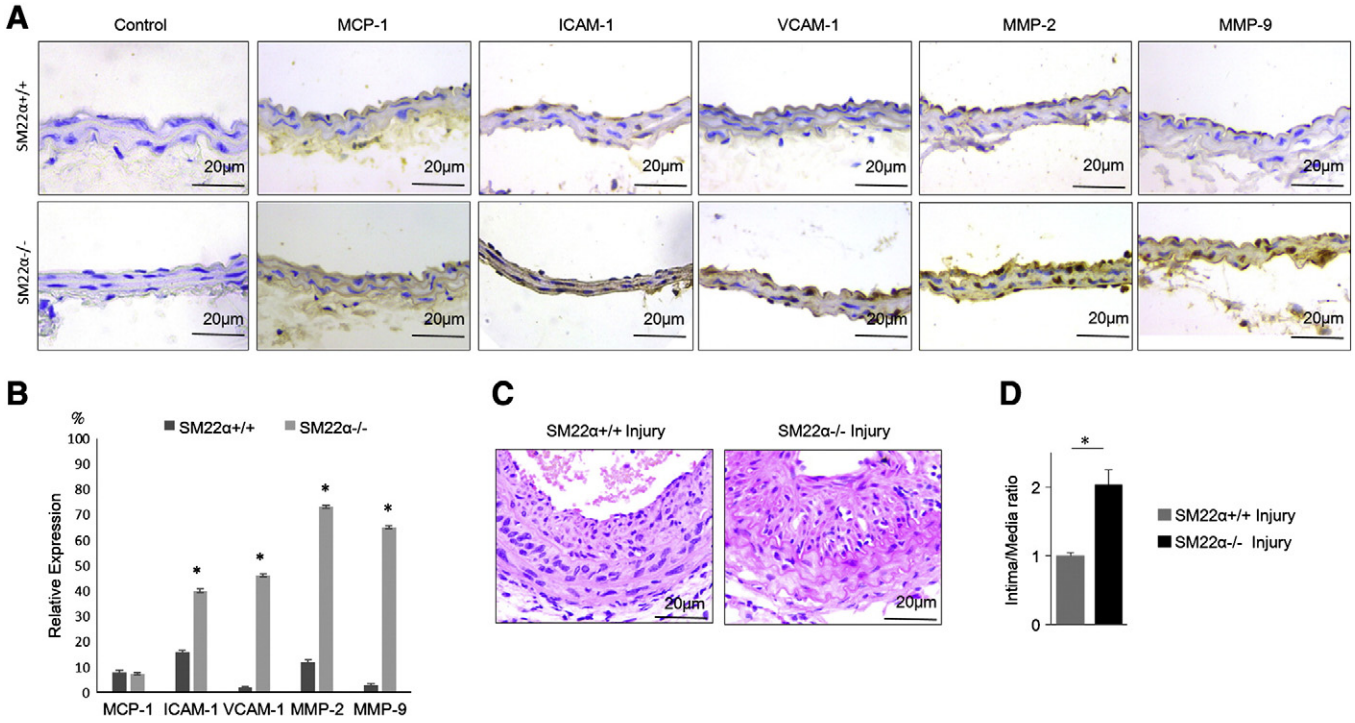

Fig. 6. SM22α$^{-/-}$ mice revealed increased tendency to develop vascular disease. A–B, Immunohistochemical staining of enriched molecules related with cellular adhesion (MCP-1, ICAM-1, and VCAM-1) and extracellular matrix degradation (MMP-2 and MMP-9) in SM22α$^{-/-}$ and SM22α$^{+/+}$ mice arteries. Student's *t* test was used to calculate the *P*-value. **P* < 0.05. C–D, Characterization the neointimal formation by partial ligation of the left carotid arteries in SM22α$^{-/-}$ and SM22α$^{+/+}$ mice by H&E staining.

triglycerides in SM22α$^{-/-}$ mice may have associations with increased levels of ApoCI. We anticipated that ApoCI affected by SM22α-knockout may contribute to accelerated atherosclerosis development, especially for the existence of injury and chronic inflammation.

Pathways and gene network analysis revealed inflammation and lipid metabolism, which are key characteristics of atherosclerosis [42,43], were significantly enriched as SM22α-knockout. Moreover, the validation of enriched genes of atherosclerosis indicated strong correlation between atherosclerosis and SM22α ablation. Cytokine tumor necrosis factor-α (TNF-α) acts as a pro-atherogenic role through the regulation of inflammatory response and lipid balance [44]. The expression levels of TNF-α in arterial walls have high correlation with the progression of atherosclerosis [45]. It promotes chemokine and adhesion molecule expression and induces VSMCs' proliferation and migration [46]. Our study showed that TNF-α was up-regulated in SM22α$^{-/-}$ mice and it may activate NF-κB nucleus translocation by PI3k-Akt pathway. IL-18 is also a potent pro-inflammatory cytokine in atherosclerosis and up-regulated in SM22α$^{-/-}$ mice [47]. Catalytic action of LPL induces the formation of atherogenic lipoprotein remnants [48]. ApoA2 is one of the most abundant proteins in HDL particles, and its overexpression induced enhanced development of aortic fatty streak lesions [49]. Both up-regulation of LPL and ApoA2 promoted the initiation of atherosclerosis. Adiponectin has protection effect from atherosclerosis [50] and its down-regulation in SM22α$^{-/-}$ mice may indicate the impaired protection function. Thus, we presumed that disruption of SM22α can accelerate vascular inflammation and disorder lipid homeostasis. NF-κB is predicted as a major upstream regulator caused by SM22α-knockout and also a key transcriptional regulator of inflammatory genes in cardiovascular diseases [51,52]. LXR-α has been recognized its crucial protective role in the initiation of a cross-talk between lipid metabolism and inflammation regarded as a prerequisite for the development of atherosclerotic lesions [53]. Critical mutations of LXR gene can dysfunction of its targeted genes that are functioned in the cross-talk between lipid peroxidation and inflammation [54]. Based on the central roles of NF-κB in inflammation and ApoCI as a node molecular of lipid metabolism in cardiovascular diseases, we selected NF-κB and LXR targeted gene ApoCI for further analysis in cultured rat VSMCs. The results showed loss of SM22α exacerbated TNF-α-mediated NF-κB activation and increased the expression levels of ApoCI in VSMCs *in vitro*, while overexpression of SM22α suppressed TNF-α-mediated NF-κB activation. As inhibition of NF-κB can be used to target atherosclerosis, SM22α may be used as a new inhibitor for NF-κB. The precise mechanisms of NF-κB and ApoCI in SM22α-mediated vascular diseases are still need to be investigated. Consequently, these characteristics not only suggest that SM22α$^{-/-}$ mice have an increased tendency to develop atherosclerosis, but also indicate SM22α actively participated in various vascular diseases. However, the atherosclerosis-susceptibility in SM22α-knockout mice *in vivo* needs to be further validated in models such as ApoE-KO or LDLR-KO mice in the future research.

From GO and PANTHER analysis of the cellular component revealed that the differentially expressed genes were chiefly G-protein coupled receptors located in plasma membrane. SM22α can bundle and stabilize actin filaments. Disruption of SM22α changed actin cytoskeletal remodeling dynamics and resulted in increased cell migration and invasion [55]. The dynamics of actin cytoskeleton is involved in the integration of multiple signaling pathways activated by both receptor tyrosine kinases (RTKs) and G protein-coupled receptors [56]. Loss of SM22α may result in prominent signal transduction alternation mediated by receptors located in membrane through cytoskeletal remodeling. Indeed, recent studies have shown that disruption of SM22α developed enhanced inflammatory responses and prominent medial chondrogenesis after carotid balloon injury [19,20]. Although the SM22α$^{-/-}$ mice didn't exhibit obvious histologically or physiological differences from the tissues of their control littermates, we presumed that some underlying molecular changes already existed. GO cellular component terms of differentially expressed genes were also related to extracellular region and cell junction. The extracellular matrix is involved in cell–cell interactions, proliferation and migration. Turnover and synthesis of extracellular matrix components play an important role in cardiovascular function [57,58]. Expression of adhesion and extracellular matrix degradation molecules is one early phase of atherosclerosis [59,60].

ICAM-1 and VCAM-1, are major adhesion molecules and play vital roles in recruiting of leukocytes to atherosclerotic lesion position [61,62]. MMP-2 and MMP-9 are prominent matrix metalloproteinases in the pathogenesis of atherosclerosis [63]. Their increased expressions in SM22α$^{-/-}$ mice may suggest the initiation of early vascular diseases such as atherosclerosis. Therefore, it is easy to understand that intimal thickness in SM22α$^{-/-}$ mice is more than that of wild type mice in the neointimal formation model. The expressions of these molecules were exacerbated in the partial ligation model of SM22α$^{-/-}$ mice (data not shown). Moreover, We have looked for evidence of SM22α involvement in vascular inflammation of human, and found that the expression of SM22α significantly decreased in the renal neointima and the carotid artery atherosclerotic plaques, accompanied by increased expression of these inflammatory molecules, compared with that of normal arteries (data not been published). These findings suggest a correlation between decreased SM22α expression and arterial diseases. These data further suggested that disruption of SM22α influenced the interaction between vascular cells and extracellular matrix, determining the phenotypic switching of VSMCs.

Other candidate genes identified by our analysis remain to be tested in the future. For example, chemokine receptors CCR3 and CXCR4 are up-regulated in the aorta of SM22α$^{-/-}$ mice. They are G-protein coupled receptors located at membrane of VSMCs and up-regulated in vascular diseases such as atherosclerosis [29,30]. Mitochondria proteins cytochrome P450 and cytochrome C oxidase were also up-regulated in SM22α$^{-/-}$ mice. Cytochrome P450 is involved in Angiotensin II-induced VSMC migration and growth [64], mitochondrial ROS generation [65] and cardiovascular inflammation [66]. We also found that the changes of some mRNA levels were not consistent with their protein levels (for example, MMP-9) and there might have other mechanisms such as protein modifications occurred. Taken together, all these information may provide novel clues for further research.

In conclusion, we used RNA-Seq to systematically investigate the global transcriptomes of the aortas in SM22α$^{-/-}$ and SM22α$^{+/+}$ mice, generating a useful resource for understanding the molecular function of SM22α. Function analysis indicated that SM22α$^{-/-}$ mice may be more sensitive to extracellular stimulation such as mechanical stimulus, hormones or growth factors. Meanwhile, our results provided evidences for the molecular basis of SM22α-related pathogenesis, and presumed that SM22α$^{-/-}$ mice may be a model of pro-atherosclerosis. Our findings suggest that SM22α can actively participate in vascular diseases, and point out some directions for our future study on SM22α functions in vascular homeostasis. Also, rescuing SM22α expression may provide a novel therapeutic strategy for arterial diseases.

Funding

This work was supported by the National Natural Science Foundation of China 31071003 and 31271222 (to M.H.), and the Program of International S&T Cooperation of China 2011DFA32700 (to M.H.).

Disclosures

None declared.

Acknowledgments

We acknowledge Liang Wang for the valuable discussions and technical support from Dalian Medical University, China.

Appendix A. Supplementary data

Supplementary data to this article can be found online at http://dx.doi.org/10.1016/j.yjmcc.2014.04.003.

References

[1] Alexander RW. Theodore Cooper Memorial Lecture. Hypertension and the pathogenesis of atherosclerosis. Oxidative stress and the mediation of arterial inflammatory response: a new perspective. Hypertension 1995;25:155–61.
[2] Gomez D, Owens GK. Smooth muscle cell phenotypic switching in atherosclerosis. Cardiovasc Res 2012;95:156–64.
[3] Owens GK, Kumar MS, Wamhoff BR. Molecular regulation of vascular smooth muscle cell differentiation in development and disease. Physiol Rev 2004;84:767–801.
[4] Gabbiani G, Schmid E, Winter S, Chaponnier C, de Ckhastonay C, Vandekerckhove J, et al. Vascular smooth muscle cells differ from other smooth muscle cells: predominance of vimentin filaments and a specific alpha-type actin. Proc Natl Acad Sci U S A 1981;78:298–302.
[5] Duband JL, Gimona M, Scatena M, Sartore S, Small JV. Calponin and SM 22 as differentiation markers of smooth muscle: spatiotemporal distribution during avian embryonic development. Differentiation 1993;55:1–11.
[6] Miano JM, Cserjesi P, Ligon KL, Periasamy M, Olson EN. Smooth muscle myosin heavy chain exclusively marks the smooth muscle lineage during mouse embryogenesis. Circ Res 1994;75:803–12.
[7] van der Loop FT, Schaart G, Timmer ED, Ramaekers FC, van Eys GJ. Smoothelin, a novel cytoskeletal protein specific for smooth muscle cells. J Cell Biol 1996;134:401–11.
[8] Papke CL, Cao J, Kwartler CS, Villamizar C, Byanova KL, Lim SM, et al. Smooth muscle hyperplasia due to loss of smooth muscle alpha-actin is driven by activation of focal adhesion kinase, altered p53 localization and increased levels of platelet-derived growth factor receptor-beta. Hum Mol Genet 2013;22:3123–37.
[9] Castro MM, Cena J, Cho WJ, Walsh MP, Schulz R. Matrix metalloproteinase-2 proteolysis of calponin-1 contributes to vascular hypocontractility in endotoxemic rats. Arterioscler Thromb Vasc Biol 2012;32:662–8.
[10] Nagai R, Kuro-o M, Aikawa M, Watanabe M, Suzuki T, Yazaki Y. Smooth muscle myosin heavy chain expression in the arterial wall; a new viewpoint for vascular pathology. Rinsho Byori 1995;43:337–41.
[11] Rensen SS, Niessen PM, van Deursen JM, Janssen BJ, Heijman E, Hermeling E, et al. Smoothelin-B deficiency results in reduced arterial contractility, hypertension, and cardiac hypertrophy in mice. Circulation 2008;118:828–36.
[12] Wamhoff BR, Hoofnagle MH, Burns A, Sinha S, McDonald OG, Owens GK. A G/C element mediates repression of the SM22alpha promoter within phenotypically modulated smooth muscle cells in experimental atherosclerosis. Circ Res 2004;95:981–8.
[13] Lenk GM, Tromp G, Weinsheimer S, Gatalica Z, Berguer R, Kuivaniemi H. Whole genome expression profiling reveals a significant role for immune function in human abdominal aortic aneurysms. BMC Genomics 2007;8:237.
[14] Puig O, Wang IM, Cheng P, Zhou P, Roy S, Cully D, et al. Transcriptome profiling and network analysis of genetically hypertensive mice identifies potential pharmacological targets of hypertension. Physiol Genomics 2010;42A:24–32.
[15] Shields JM, Rogers-Graham K, Der CJ. Loss of transgelin in breast and colon tumors and in RIE-1 cells by Ras deregulation of gene expression through Raf-independent pathways. J Biol Chem 2002;277:9790–9.
[16] Prasad PD, Stanton JA, Assinder SJ. Expression of the actin-associated protein transgelin (SM22) is decreased in prostate cancer. Cell Tissue Res 2010;339:337–47.
[17] Xie XL, Liu YB, Liu YP, Du BL, Li Y, Han M, et al. Reduced expression of SM22 is correlated with low autophagy activity in human colorectal cancer. Pathol Res Pract 2013;209:237–43.
[18] Feil S, Hofmann F, Feil R. SM22alpha modulates vascular smooth muscle cell phenotype during atherogenesis. Circ Res 2004;94:863–5.
[19] Shen J, Yang M, Ju D, Jiang H, Zheng JP, Xu Z, et al. Disruption of SM22 promotes inflammation after artery injury via nuclear factor kappaB activation. Circ Res 2010;106:1351–62.
[20] Shen J, Yang M, Jiang H, Ju D, Zheng JP, Xu Z, et al. Arterial injury promotes medial chondrogenesis in Sm22 knockout mice. Cardiovasc Res 2011;90:28–37.
[21] Dong LH, Wen JK, Liu G, McNutt MA, Miao SB, Gao R, et al. Blockade of the Ras-extracellular signal-regulated kinase 1/2 pathway is involved in smooth muscle 22 alpha-mediated suppression of vascular smooth muscle cell proliferation and neointima hyperplasia. Arterioscler Thromb Vasc Biol 2010;30:683–91.
[22] Lv P, Miao SB, Shu YN, Dong LH, Liu G, Xie XL, et al. Phosphorylation of smooth muscle 22alpha facilitates angiotensin II-induced ROS production via activation of the PKCdelta-P47phox axis through release of PKCdelta and actin dynamics and is associated with hypertrophy and hyperplasia of vascular smooth muscle cells in vitro and in vivo. Circ Res 2012;111:697–707.
[23] Trapnell C, Pachter L, Salzberg SL. TopHat: discovering splice junctions with RNA-Seq. Bioinformatics 2009;25:1105–11.
[24] Trapnell C, Williams BA, Pertea G, Mortazavi A, Kwan G, van Baren MJ, et al. Transcript assembly and quantification by RNA-Seq reveals unannotated transcripts and isoform switching during cell differentiation. Nat Biotechnol 2010;28:511–5.
[25] Huang da W, Sherman BT, Lempicki RA. Systematic and integrative analysis of large gene lists using DAVID bioinformatics resources. Nat Protoc 2009;4:44–57.
[26] Huang da W, Sherman BT, Lempicki RA. Bioinformatics enrichment tools: paths toward the comprehensive functional analysis of large gene lists. Nucleic Acids Res 2009;37:1–13.
[27] Mi H, Muruganujan A, Thomas PD. PANTHER in 2013: modeling the evolution of gene function, and other gene attributes, in the context of phylogenetic trees. Nucleic Acids Res 2013;41:D377–86.
[28] Nam D, Ni CW, Rezvan A, Suo J, Budzyn K, Llanos A, et al. Partial carotid ligation is a model of acutely induced disturbed flow, leading to rapid endothelial dysfunction and atherosclerosis. Am J Physiol Heart Circ Physiol 2009;297:H1535–43.
[29] Jie W, Wang X, Zhang Y, Guo J, Kuang D, Zhu P, et al. SDF-1alpha/CXCR4 axis is involved in glucose-potentiated proliferation and chemotaxis in rat vascular smooth muscle cells. Int J Exp Pathol 2010;91:436–44.

[30] Kodali RB, Kim WJ, Galaria II, Miller C, Schecter AD, Lira SA, et al. CCL11 (Eotaxin) induces CCR3-dependent smooth muscle cell migration. Arterioscler Thromb Vasc Biol 2004;24:1211–6.
[31] Zhan M, Yuan F, Liu H, Chen H, Qiu X, Fang W. Inhibition of proliferation and apoptosis of vascular smooth muscle cells by ghrelin. Acta Biochim Biophys Sin (Shanghai) 2008;40:769–76.
[32] Tan HW, Liu X, Bi XP, Xing SS, Li L, Gong HP, et al. IL-18 overexpression promotes vascular inflammation and remodeling in a rat model of metabolic syndrome. Atherosclerosis 2010;208:350–7.
[33] Kanters E, Pasparakis M, Gijbels MJ, Vergouwe MN, Partouns-Hendriks I, Fijneman RJ, et al. Inhibition of NF-kappaB activation in macrophages increases atherosclerosis in LDL receptor-deficient mice. J Clin Invest 2003;112:1176–85.
[34] Diez D, Wheelock AM, Goto S, Haeggstrom JZ, Paulsson-Berne G, Hansson GK, et al. The use of network analyses for elucidating mechanisms in cardiovascular disease. Mol Biosyst 2010;6:289–304.
[35] Shachter NS. Apolipoproteins C-I and C-III as important modulators of lipoprotein metabolism. Curr Opin Lipidol 2001;12:297–304.
[36] Westerterp M, Berbee JF, Pires NM, van Mierlo GJ, Kleemann R, Romijn JA, et al. Apolipoprotein C-I is crucially involved in lipopolysaccharide-induced atherosclerosis development in apolipoprotein E-knockout mice. Circulation 2007;116:2173–81.
[37] Dumont L, Gautier T, de Barros JP, Laplanche H, Blache D, Ducoroy P, et al. Molecular mechanism of the blockade of plasma cholesteryl ester transfer protein by its physiological inhibitor apolipoprotein CI. J Biol Chem 2005;280:38108–16.
[38] Nagelkerken L, Verzaal P, Lagerweij T, Persoon-Deen C, Berbee JF, Prens EP, et al. Development of atopic dermatitis in mice transgenic for human apolipoprotein C1. J Invest Dermatol 2008;128:1165–72.
[39] Berbee JF, van der Hoogt CC, Sundararaman D, Havekes LM, Rensen PC. Severe hypertriglyceridemia in human APOC1 transgenic mice is caused by apoC-I-induced inhibition of LPL. J Lipid Res 2005;46:297–306.
[40] Joh JHEH, Kim DI. Expression of apoC1 and FTL genes in human with carotid atherosclerosis. J Korean Surg Soc 2006;1:56–60.
[41] Chang CT, Liao HY, Chang CM, Chen CY, Chen CH, Yang CY, et al. Oxidized ApoC1 on MALDI-TOF and glycated-ApoA1 band on gradient gel as potential diagnostic tools for atherosclerotic vascular disease. Clin Chim Acta 2013;420:69–75.
[42] Libby P, Ridker PM, Hansson GK. Progress and challenges in translating the biology of atherosclerosis. Nature 2011;473:317–25.
[43] van Diepen JA, Berbee JF, Havekes LM, Rensen PC. Interactions between inflammation and lipid metabolism: relevance for efficacy of anti-inflammatory drugs in the treatment of atherosclerosis. Atherosclerosis 2013;228:306–15.
[44] McKellar GE, McCarey DW, Sattar N, McInnes IB. Role for TNF in atherosclerosis? Lessons from autoimmune disease. Nat Rev Cardiol 2009;6:410–7.
[45] Zhang Y, Yang X, Bian F, Wu P, Xing S, Xu G, et al. TNF-α promotes early atherosclerosis by increasing transcytosis of LDL across endothelial cells: crosstalk between NF-κB and PPAR-γ. J Mol Cell Cardiol 2014;72:85–94.
[46] Zhang L, Peppel K, Sivashanmugam P, Orman ES, Brian L, Exum ST, et al. Expression of tumor necrosis factor receptor-1 in arterial wall cells promotes atherosclerosis. Arterioscler Thromb Vasc Biol 2007;27:1087–94.
[47] Elhage R, Jawien J, Rudling M, Ljunggren HG, Takeda K, Akira S, et al. Reduced atherosclerosis in interleukin-18 deficient apolipoprotein E-knockout mice. Cardiovasc Res 2003;59:234–40.
[48] Mead JR, Ramji DP. The pivotal role of lipoprotein lipase in atherosclerosis. Cardiovasc Res 2002;55:261–9.
[49] Warden CH, Daluiski A, Bu X, Purcell-Huynh DA, De Meester C, Shieh BH, et al. Evidence for linkage of the apolipoprotein A-II locus to plasma apolipoprotein A-II and free fatty acid levels in mice and humans. Proc Natl Acad Sci U S A 1993;90:10886–90.
[50] Yamauchi T, Kamon J, Waki H, Imai Y, Shimozawa N, Hioki K, et al. Globular adiponectin protected ob/ob mice from diabetes and ApoE-deficient mice from atherosclerosis. J Biol Chem 2003;278:2461–8.
[51] Lawrence T. The nuclear factor NF-kappaB pathway in inflammation. Cold Spring Harb Perspect Biol 2009;1:a001651.
[52] Hall G, Hasday JD, Rogers TB. Regulating the regulator: NF-kappaB signaling in heart. J Mol Cell Cardiol 2006;41:580–91.
[53] Calkin AC, Tontonoz P. Liver x receptor signaling pathways and atherosclerosis. Arterioscler Thromb Vasc Biol 2010;30:1513–8.
[54] Dave VP, Kaul D, Sharma Y, Bhattacharya R. Functional genomics of blood cellular LXR-alpha gene in human coronary heart disease. J Mol Cell Cardiol 2009;46:536–44.
[55] Thompson O, Moghraby JS, Ayscough KR, Winder SJ. Depletion of the actin bundling protein SM22/transgelin increases actin dynamics and enhances the tumourigenic phenotypes of cells. BMC Cell Biol 2012;13:1.
[56] Gerthoffer WT. Mechanisms of vascular smooth muscle cell migration. Circ Res 2007;100:607–21.
[57] Berk BC, Fujiwara K, Lehoux S. ECM remodeling in hypertensive heart disease. J Clin Invest 2007;117:568–75.
[58] Bowers SL, Banerjee I, Baudino TA. The extracellular matrix: at the center of it all. J Mol Cell Cardiol 2010;48:474–82.
[59] Blankenberg S, Barbaux S, Tiret L. Adhesion molecules and atherosclerosis. Atherosclerosis 2003;170:191–203.
[60] Katsuda S, Kaji T. Atherosclerosis and extracellular matrix. J Atheroscler Thromb 2003;10:267–74.
[61] Ley K, Huo Y. VCAM-1 is critical in atherosclerosis. J Clin Invest 2001;107:1209–10.
[62] Nakashima Y, Raines EW, Plump AS, Breslow JL, Ross R. Upregulation of VCAM-1 and ICAM-1 at atherosclerosis-prone sites on the endothelium in the ApoE-deficient mouse. Arterioscler Thromb Vasc Biol 1998;18:842–51.
[63] Caird J, Napoli C, Taggart C, Farrell M, Bouchier-Hayes D. Matrix metalloproteinases 2 and 9 in human atherosclerotic and non-atherosclerotic cerebral aneurysms. Eur J Neurol 2006;13:1098–105.
[64] Yaghini FA, Song CY, Lavrentyev EN, Ghafoor HU, Fang XR, Estes AM, et al. Angiotensin II-induced vascular smooth muscle cell migration and growth are mediated by cytochrome P450 1B1-dependent superoxide generation. Hypertension 2010;55:1461–7.
[65] Clempus RE, Griendling KK. Reactive oxygen species signaling in vascular smooth muscle cells. Cardiovasc Res 2006;71:216–25.
[66] Deng Y, Theken KN, Lee CR. Cytochrome P450 epoxygenases, soluble epoxide hydrolase, and the regulation of cardiovascular inflammation. J Mol Cell Cardiol 2010;48:331–41.